1-1-2008

The effective interdiffusivity, structure, and magnetic properties of Fe/Pt (n) multilayer films

Bo Yao
University of Central Florida

Kevin R. Coffey
University of Central Florida

The effective interdiffusivity, structure, and magnetic properties of $[Fe/Pt]_n$ multilayer films

Cite as: J. Appl. Phys. **103**, 07E107 (2008); https://doi.org/10.1063/1.2828978
Submitted: 07 September 2007 . Accepted: 27 September 2007 . Published Online: 22 January 2008

Bo Yao, and Kevin R. Coffey

The effective interdiffusivity, structure, and magnetic properties of $[Fe/Pt]_n$ multilayer films

Bo Yao[a] and Kevin R. Coffey
Advanced Materials Processing and Analysis Center and Department of Mechanical, Materials and Aerospace Engineering, University of Central Florida, Orlando, Florida 32816, USA

(Presented on 9 November 2007; received 7 September 2007; accepted 27 September 2007; published online 22 January 2008)

This paper reports the influence of the deposition temperature and the wavelength of the periodicity on the effective interdiffusivity, microstructure, and magnetic properties of annealed $[Fe/Pt]_n$ multilayer films (MLs). It was found that both the deposition temperature and periodicity of $[Fe/Pt]_n$ MLs have a significant influence on the effective Fe–Pt interdiffusivity, microstructure, and magnetic properties of the annealed films. It was also observed that the magnitude of the effective interdiffusion coefficient, the $L1_0$ grain size, and the long-range order parameter were positively correlated. This result suggests that nonequilibrium reaction kinetics are desirable for the reduced temperature formation of the $L1_0$ FePt phase. © *2008 American Institute of Physics*.
[DOI: 10.1063/1.2828978]

I. INTRODUCTION

The $L1_0$ FePt phase has received research interest because of its potential application for high-density magnetic recording media and high-energy permanent magnets, mainly due to its large magnetocrystalline anisotropy energy density ($K_u \sim 10^7$ ergs/cm^3).[1] For many potential applications it is desirable to obtain the ordered $L1_0$ phase at a minimal processing temperature. Multiple layers of elemental Fe and Pt films, $[Fe/Pt]_n$, have attracted attention, due to the observation of the $L1_0$ FePt phase at reduced annealing temperatures, as low as 300 °C for both epitaxial[2–6] and polycrystalline[7,8] films. Although the mechanism of this reaction is still poorly understood, the rapid interdiffusion of Fe and Pt at the interface is generally believed to be responsible for the formation of $L1_0$ FePt. Efforts[4,9–11] have been made to measure the bulk Fe–Pt interdiffusivity and to understand the relationship between interdiffusivity and formation of $L1_0$ FePt phase. However, it has been demonstrated in both theory and experiments that the effective interdiffusivity (D_Λ) in nanoscale multilayer films (MLs) can deviate significantly from the bulk interdiffusivity due to the influence of the steep composition gradient and coherent strains in MLs.[12–16] Therefore, it may not be useful to use the measured bulk diffusivity to understand the interdiffusion of MLs.

Instead, the effective interdiffusivity in MLs can be directly determined from the decay rate of the intensity of small angle x-ray diffraction (XRD) peaks due to thermal treatments. The repetitive layer pairs of different x-ray scattering strength in the MLs induce small angle XRD peaks around the (000) reflection (direct beam), and the decay of these peaks due to annealing is directly related to the homogenization of these compositionally modulated layers. The effective interdiffusivity D_Λ is given by the decay rate of the first small angle peak intensity $I(t)$ during annealing (reviewed in Ref. 17):

$$D_\Lambda = -[\Lambda^2/(8\pi^2)]d\{\ln[I(t)/I(0)]\}/dt, \quad (1)$$

where $I(0)$ is the initial intensity of as-deposited films, Λ is the bilayer period (i.e., sum of the thickness of a single Pt and a single Fe layer), and t is the annealing time. The values of $I(t)$ and $I(0)$ can be measured through small angle XRD, and the values of t and Λ are known. This method has been applied to measure the interdiffusivity of a large variety of material systems such as Si/SiG,[18,19] Mo/Si,[20] Cu/Pd,[15] GaAs/AlAs,[21] and Au/Ag (Ref. 16) MLs. Most recently, Se-Young *et al.*[22] and Zotov *et al.*[17] used this approach to measure the effective Fe–Pt interdiffusivity of $[Fe/Pt]_n$ MLs. Interestingly, they found that the effective interdiffusivity differed for different Fe–Pt MLs, which, in part, motivates this more comprehensive study.

The aim of this paper is to investigate the influence of the deposition temperature and the wavelength of the periodicity of the $[Fe/Pt]_n$ MLs on the effective interdiffusivity, microstructure, and magnetic properties of the films after annealing. As will be shown, both the deposition temperature and periodicity of $[Fe/Pt]_n$ MLs have a significant influence on the effective Fe–Pt interdiffusivity and upon the microstructure and magnetic properties of the annealed films. It was also found that the magnitude of the effective interdiffusion coefficient, the $L1_0$ grain size, and the long-range order parameter were positively correlated. This result suggests that nonequilibrium reaction kinetics are desirable for the reduced temperature formation of the $L1_0$ FePt phase.

II. EXPERIMENTS

Two sets of $[Fe/Pt]_n$ samples were sputtered on oxidized Si substrates, as listed in Table I. The first set of samples (labeled as "a," "b," "c," "d," and "e") have the same layer structure, $[Fe_{22\ Å}Pt_{28\ Å}]_{12}$ but different deposition substrate

[a]Electronic mail: bo555252@pegasus.cc.ucf.edu.

TABLE I. A list of $[Fe/Pt]_n$ MLs.

Sample label	Multilayer structure	Period (Å)	Depo. temp. (°C)
a	$[Fe_{22\ Å}Pt_{28\ Å}]_{12}$	50	−50
b	$[Fe_{22\ Å}Pt_{28\ Å}]_{12}$	50	25
c	$[Fe_{22\ Å}Pt_{28\ Å}]_{12}$	50	150
d	$[Fe_{22\ Å}Pt_{28\ Å}]_{12}$	50	200
e	$[Fe_{22\ Å}Pt_{28\ Å}]_{12}$	50	250
f	$[Fe_{5\ Å}Pt_{6.4\ Å}]_{48}$	11.4	250
g	$[Fe_{10\ Å}Pt_{12.8\ Å}]_{24}$	22.8	250
h	$[Fe_{20\ Å}Pt_{25.6\ Å}]_{12}$	45.6	250
i	$[Fe_{40\ Å}Pt_{51.3\ Å}]_{6}$	91.3	250
j	$[Fe_{80\ Å}Pt_{102.6\ Å}]_{3}$	182.6	250

temperatures, in the range of −50–250 °C. Among them, samples a, b, and d were selected to examine the influence of deposition temperature on the effective interdiffusion coefficient. The second set of samples, labeled as "f," "g," "h," "i," and "j," have a common deposition temperature, 250 °C, but varying periodicity, in the range of 11.4–182.6 Å. Among them, samples g, h, and i were chosen to determine the influence of periodicity on the interdiffusivity. The details of the ML sample preparation have been previously reported.[23] The ML film samples were annealed in a modified tube furnace in 1 atm of flowing Ar+5% H_2 process gas, described also in Ref. 23. The modified furnace allows a rapid heating and cooling of samples without breaking the annealing ambient.

Small angle XRD patterns were acquired in a RigaKu x-ray diffraction instrument with a Cu $K\alpha$ source. Magnetic properties were measured with an alternate gradient force magnetometer (Princeton Measurements Corp. MicroMag model 2900) with a maximum field of 22 kOe. The microscopy was performed in a Tecnai F30 microscope operating at 300 kV. Hollow-cone annual dark field (ADF) transmission electron microscopy (TEM) images were used to analyze the structure of $L1_0$ phase. The TEM samples were prepared using a back-etch technique.

III. RESULTS AND DISCUSSION

Small angle XRD patterns confirm that the multilayer structures were preserved in good condition for all as-deposited samples.[23] Figure 1(a) shows the evolution of the small angle x-ray diffraction pattern for sample i (a representative example) annealed for different times at 325 °C. The intensity of the satellite peak decreases with annealing time due to the interdiffusion of Fe and Pt at the interface. Figure 1(b) shows plots of $\ln[I(t)/I(0)]$ versus t for samples g, h, and i annealed for different times at 325 °C. It can be seen that $\ln[I(t)/I(0)]$ falls almost linearly with the annealing time after the first anneal. The fitted lines do not meet the Y axis at 0, due to an initial drop in intensity, which has been widely observed and investigated in many systems.[17] As a common practice, the linear decay after the initial rapid drop is taken to determine the effective interdiffusivity for each sample at the annealing temperature studied.

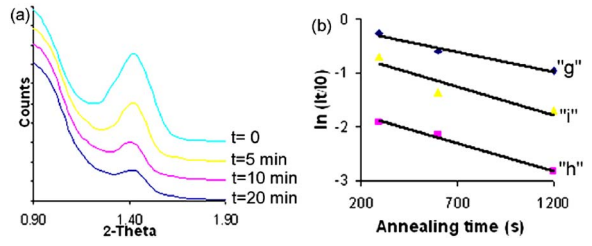

FIG. 1. (Color online) (a) The decay of the first satellite peak due to annealing for sample "i" annealed at 325 °C. (b) The plots of $\ln[I(t)/I(0)]$ vs annealing time (t) for samples "g," "h," and "i" annealed for different times at 325 °C.

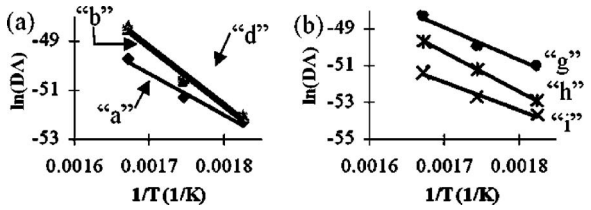

FIG. 2. (a) The $\ln(D_\Lambda)$ vs $(1/T)$ for samples "a," "b," and "d." (b) The $\ln(D_\Lambda)$ vs $(1/T)$ for samples "g," "h," and "i." D_Λ has the unit of m^2/s.

All six samples (a, b, d, and g, h, i) were annealed for different times at 275, 300, and 325 °C. The measured effective interdiffusivities, according to Eq. (1), are shown in Fig. 2 in the form of $\ln(D_\lambda)$ plotted as a function of $1/T$. It can be seen from Fig. 2(b) that the effective interdiffusivity increases with the increase of periodicity for samples g, h, and i, with approximately similar interdiffusion activation energies (ranging from 1.3 to 1.8 eV). This trend is consistent with the greater effective interdiffusivity reported for larger periodicity Fe/Pt MLs by Zotov *et al.*[17] In the set of samples deposited at different temperatures, as shown in Fig. 2(a), sample a (deposited at −50 °C) has a lower interdiffusivity and activation energy, while the effective interdiffusivity of samples b and d is similar in magnitude and temperature dependence (activation energy).

Figures 3(a) and 3(b) show the measured in-plane coercivity for samples annealed at 400 and 500 °C. The results show that both the deposition temperature and periodicity of films have a great influence on this magnetic property. More interestingly, by comparing the coercivities (Fig. 3) and interdiffusivities (Fig. 2) for the two sets of samples, it can be noted that samples having large effective interdiffusivities generally have large coercivity. To further understand these films, hollow-cone ADF TEM microscopy and electron dif-

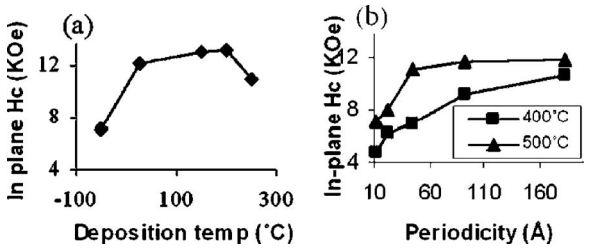

FIG. 3. (a) The in-plane Hc vs deposition temperature for samples "a," "b," "c," "d," and "e." All samples were annealed at 500 °C for 30 min. (b) The in-plane Hc vs periodicity for samples "f," "g," "h," "i," and "j" annealed at temperatures of 400 and 500 °C for 30 min.

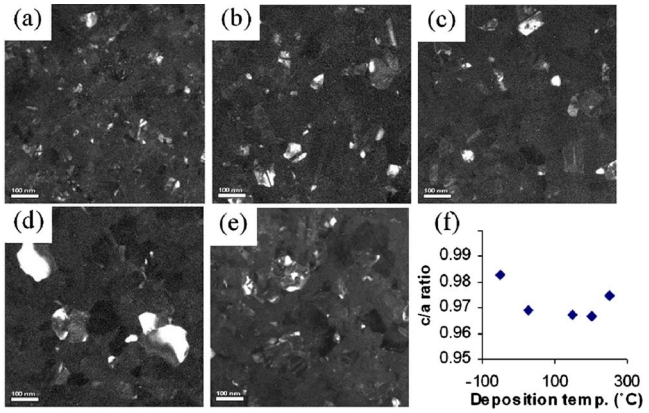

FIG. 4. (Color online) [(a)–(e)] ADF TEM images from $L1_0$ (001) and (110) superlattice reflections of samples "a," "b," "c," "d," and "e" annealed at 500 °C for 30 min. (f) The c/a ratio vs deposition temperature. The bar shows 100 nm.

fraction studies were undertaken to examine the structure of $L1_0$ FePt phase and its long-range order parameter in these samples.

The as-deposited films were found to consist of fcc phase Fe and Pt (except samples i and j which have a bcc phase Fe present) while the annealed films showed evidence of both fcc and $L1_0$ phases, but lacked evidence of the Fe_3Pt and $FePt_3$ $L1_2$ phases that have been reported by others in much larger periodicity Fe/Pt MLs.[2] We hypothesize that the absence of the $L1_2$ phases is due to a lack of driving force for their nucleation in our small periodicity samples. Figures 4(a)–4(e) show the hollow-cone ADF TEM images from the (001) and (110) superlattice reflections of samples a, b, c, d, and e, respectively, annealed at 500 °C for 30 min. The illuminated regions in the images show the $L1_0$ FePt grains with (001) or (110) planes parallel to the electron beam. Figure 4(f) shows the c/a ratio of the $L1_0$ phase of these five annealed samples. Figures 5(a)–5(e) show the ADF TEM images from the (001) and (110) $L1_0$ superlattice reflections for samples f, g, h, i, and j, respectively, annealed at 500 °C for 30 min. Figure 5(f) shows the c/a ratio of the $L1_0$ phase of these five annealed samples. It can be noted from examination of Figs. 4 and 5 that both a larger grain size and a lower

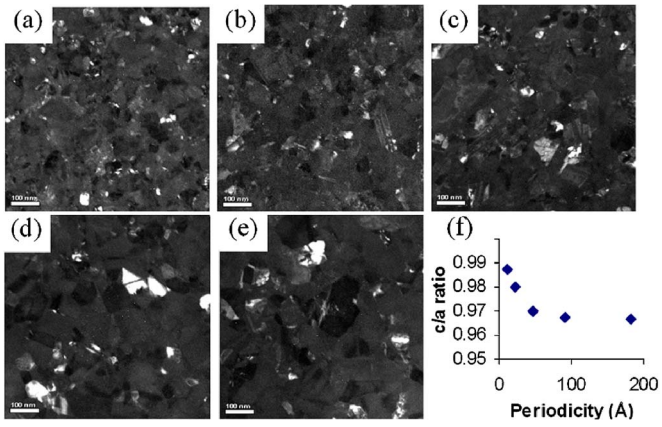

FIG. 5. (Color online) [(a)–(e)] ADF TEM images from $L1_0$ (001) and (110) superlattice reflections of samples "f," "g," "h," "i," and "j" annealed at 500 °C for 30 min. (f) The c/a ratio vs deposition temperature. The bar shows 100 nm.

c/a ratio of $L1_0$ FePt phase (indicating a greater value for the chemical order parameter[24]) are observed for samples having higher effective interdiffusivities (Fig. 2) and in-plane coercivities (Fig. 3). Specifically, samples with larger interdiffusivities generally have larger $L1_0$ FePt grains, larger long-range order parameters (indicated by small c/a ratio), and larger coercivities. This correlation of structural and magnetic properties to the effective interdiffusivity suggests that nonequilibrium reaction kinetics are desirable for the reduced temperature formation of the $L1_0$ FePt phase.

IV. CONCLUSIONS

This paper reports the influence of the deposition temperature and the wavelength of the periodicity of $[Fe/Pt]_n$ MLs on the effective interdiffusivity, microstructure, and magnetic properties of the films after annealing. It was found that both the deposition temperature and periodicity of $[Fe/Pt]_n$ MLs have a significant influence on the effective Fe–Pt interdiffusivity, microstructure, and magnetic properties of the annealed films. It was also observed that the magnitude of the effective interdiffusion coefficient, the $L1_0$ grain size, and the long-range order parameter were positively correlated. In all cases studied, the $L1_2$ phases were bypassed. This result suggests that nonequilibrium reaction kinetics are desirable for the reduced temperature formation of the $L1_0$ FePt phase.

[1] R. Skomski, J. Phys.: Condens. Matter **15**, R841 (2003).
[2] M. Verdier, M. Veron, F. Bley, F. Ingwiller, N. M. Dempsey, and D. Givord, Philos. Mag. **85**, 3157 (2005).
[3] Y. Endo, N. Kikuchi, O. Kitakami, and Y. Shimada, J. Appl. Phys. **89**, 7065 (2001).
[4] Y. Endo, K. Oikawa, T. Miyazaki, O. Kitakami, and Y. Shimada, J. Appl. Phys. **94**, 7222 (2003).
[5] S. C. Chou, C. C. Yu, Y. Liou, and Y. D. Yao, Phys. Status Solidi A **201**, 1755 (2004).
[6] S. C. Chou, C. C. Yu, Y. Liou, Y. D. Yao, D. H. Wei, T. S. Chin, and M. F. Tai, J. Appl. Phys. **95**, 7276 (2004).
[7] C. P. Luo and D. J. Shellmyer, IEEE Trans. Magn. **31**, 2764 (1995).
[8] V. Raghavendra Reddy, S. Kavita, and A. Gupta, J. Appl. Phys. **99**, 113906 (2006).
[9] H. Mehrer, *Diffusion in Solid Metals and Alloys*, Landolt-Bornstein, New Series, Group III, Vol. 26 (Springer, Berlin, 1990).
[10] Kushida, K. Tanaka, and H. Numakura, Mater. Trans. **44**, 59 (2003).
[11] Y. Nose, T. Ikeda, H. Nakajima, and H. Numakura, Defect Diffus. Forum **237–240**, 450 (2005).
[12] A. Lindsay Greer, Curr. Opin. Solid State Mater. Sci. **2**, 300 (1997).
[13] L. Chang and B. C. Giessen, *Synthetic Modulated Structures* (Academic, New York, 1985).
[14] D. Gupta and P. S. Ho, *Diffusion Phenomena in Thin Films and Microelectronic Materials* (Noyes, Park Ridge, NJ, 1988).
[15] E. M. Philofsky and J. E. Hilliard, J. Appl. Phys. **40**, 2198 (1969).
[16] H. E. Cook and J. E. Hilliard, J. Appl. Phys. **40**, 2191 (1969).
[17] N. Zotov, J. Feydt, A. Savan, and A. Ludwig, J. Appl. Phys. **100**, 073517 (2006).
[18] S. M. Prokes, M. Fatemi, and K. L. Wang, J. Vac. Sci. Technol. B **8**, 254 (1990).
[19] D. B. Aubertine, N. Ozguveen, P. C. McIntyre, and S. Brenan, J. Appl. Phys. **94**, 1557 (2003).
[20] H. Nakajima and H. Fujimori, J. Appl. Phys. **63**, 1046 (1988).
[21] R. M. Fleming, D. B. McWhan, A. C. Gossard, W. Wiegmann, and R. A. Logan, J. Appl. Phys. **51**, 357 (1980).
[22] O. Se-Young, D. P. Nguyen, C. G. Lee, B. S. Lee, B. H. Koo, H. Y. Liu, J. H. Yoo, and K. Shin, Diffus. Defect Data, Pt. A **258–260**, 199 (2006).
[23] B. Yao and K. R. Coffey, J. Magn. Magn. Mater. **320**, 559 (2008).
[24] B. W. Roberts, Acta Metall. **2**, 597 (1954).